Effect of substrate rigidity on distribution of nuclear actin and lamin A

Tommi Ijäs
Master's thesis
University of Jyväskylä
Department of Biological and Environmental Sciences
Cell and molecular biology
21.5.2016

PREFACE

This work was performed at University of Tampere BioMediTech department under the guidance of Teemu Ihalainen. I would like to express my deepest gratitude to my primary supervisor Teemu Ihalainen, who gave me the opportunity to work with him and taught the basics needed for this study. I also appreciate the help with the practical matters and planning of the trip from my co-supervisor Janne Ihalainen from University of Jyväskylä. I would also like to thank Vesa Hytönen and his group at BioMediTech for giving access to their laboratory and helping with the work.

20.4.2016

Tommi Ijäs

Jyväskylän yliopisto **Pro gradu tutkielman tiivistelmä**
Matemaatis-luonnontieteellinen tiedekunta

Tekijä: Tommi Ijäs
Tutkielman nimi: Alustan jäykkyyden vaikutus aktiinin ja lamiini A:n tuman sisäiseen sijoittumiseen
English title: Effect of substrate rigidity on distribution o f nuclear actin and lamin A
Päivämäärä: 21.5.2016 **Sivumäärä:** 39

Laitos: Bio- ja ympäristötieteiden laitos
Oppiaine: Solu- ja molekyylibiologia
Tutkielman ohjaajat: Teemu Ihalainen ja Janne Ihalainen

Tiivistelmä:

Tämä tutkimus keskittyi analysoimaan, onko solun ulkopuolisen ympäristön jäykkyydellä vaikutusta tuman sisäisten proteiinien jakautumiseen. Tuman mekanosensitiivisyyden vaikutusta lamiini A:n ja aktiinin sijaintiin tumassa tutkittiin soluilla, joita kasvatettiin eri jäykkyisillä kasvualustoilla. Kokeissa laskettiin lamiini A:n suhteellinen määrä vertaamalla tumalevyyn sitoutunutta ja tumassa vapaana olevaa lamiini A:ta, sekä suhteellinen määrä aktiinille vertaamalla tumansisäisen aktiinin määrää solulimassa olevaan. Kahta eri jäykkyistä (1,5 kPa ja 33 kPa Youngin moduluksella) polyakryyliamidi (PAA)-geeliä käytettiin säädettävänä kasvualustana soluille.

Näillä geeleillä kasvatettiin hiiren 3T3 fibroblastisoluja, joihin oli transfektoitu konstrukti, joka ilmentää joko lamiini A:ta tai aktiinia tehostetulla vihreällä fluoresoivalla proteiinilla (EGFP) leimattuna. Proteiineja ilmentäviä soluja kuvannettiin laser-skannaus konfokaalimikroskoopilla. Data käsiteltiin ja analysoitiin imageJ-ohjelmalla ja lopulliset tulokset saatiin vertaamalla tuman sisäistä vapaata lamiini A:ta tumalevyyn sistoutuneeseen, sekä aktiinille vertaamalla tuman sisäisen aktiinin intensiteettiä solulimasta saatuun intensiteettiin.

Lamiini A:lle tulokset näyttivät, että suurempi jäykkyys vaikuttaa lamiini A:n dynamiikkaan suurentamalla tumalimassa vapaana olevan lamiini A:n määrää suhteessa tumalevyyn sitoutuneeseen. Aktiinille tulokset olivat vähemmän yhteneviä tutkimuksen aikana, mutta myös tumansisäisen aktiinin määrä vaikuttaisi kasvavan jäykemmällä alustalla suhteutettuna soluliman aktiinipitoisuuteen. Lamiini A:n suhteen on kuitenkin näytetty että sen kokonaispitoisuus kasvaa ja fosforyloidun lamiini A:n määrä vähenee kun solu on jäykemmässä ympäristössä. Vaikka nämä tulokset eivät suoranaisesti tuekkaan toisiaan, osoitettiin tutkimuksessa alustan jäykkyyden vaikuttavan sitoutuneen ja vapaan lamiini A:n suhteeseen. Aktiinista saadut tulokset tukevat tietoja aktiinin aktiivisen tumakuljetuksen kasvamisesta kun solu joutuu rasituksen alaiseksi. Molemmat tulokset kuitenkin osoittavat jäykkyydellä olevan suora vaikutus tuman proteiinien dynamiikkaan.

Avainsanat: lamiini A, aktiini, tumakalvo, tumansisäinen, PAA-geeli

University of Jyväskylä
Faculty of Mathematics and Science

Abstract of Master's Thesis

Author: Tommi Ijäs
Title of thesis: Effect of susbstrate rigidity on distribution o f nuclear actin and lamin A
Finnish title: Alustan jäykkyyden vaikutus aktiinin ja lamiini A:n tuman sisäiseen sijoittumiseen
Date: 21.5.2016 **Pages:** 39

Department: Department of Biological and Environmental Sciences
Chair: Cell and Molecular Biology
Supervisors: Teemu Ihalainen and Janne Ihalainen

Abstract

In this study we aimed to see if the rigidity of the extracellular environment can influence protein distribution within the nucleus. The effect of nuclear mechanosensing on the spatial localization of lamin A and actin was studied in cells cultured on different rigidity cell culture substrates. We quantified the relative levels of lamin A in nuclear lamina vs. nucleoplasm and the amount of intranuclear actin vs. cytoplasmic actin. Two different rigidities (1.5 kPa and 33 kPa of Young's modulus) of polyacrylamide (PAA)-gels were used as a tunable substrate for the cells.

On these gels, we cultured mouse 3T3 fibroblast cells, which were transfected with enhanced green fluorescent protein (EGFP) labeled lamin A and actin. Cultured cells we imaged with laser scanning confocal microscope. Images were processed and analyzed using imageJ and comparisons were made between mean intensities of lamin A in the nuclear lamina and nucleoplasm, and between intranuclear and cytoplasmic actin.

With lamin A, the results showed that a higher rigidity affects lamin A dynamics, by a significant increase of free lamin A in relation to bound lamin A. With actin, the results were more unclear, but the same trend seems to continue. Actin amount inside nucleus seemed to increase related to cytoplasmic actin, when the cells were cultured on more rigid substrate. In both cases, substrate rigidity affected the protein dynamics by increasing free protein inside nucleus. Actin also seems to be actively taken into nucleus in larger quantities in more rigid environment. It has been recently shown that stiffer substrate increases lamin A amount and decreases phosphorylated lamin A, which might contradict our results. The effect of substrate rigidity on actin regulation is still poorly understood, but our results seem to be in line with proposed actin active intake to nucleus at cellular stress. Still, both of these results signify that cells have more direct mechanisms of sensing inside nucleus to affect nuclear activities.

Keywords: lamin A, actin, nuclear membrane, internuclear, PAA-gel

Table of Contents

ABBREVIATIONS

ARP	actin-related protein
APTES	(3-Aminopropyl)triethoxysilane
BAF	barrier-to-autointegration factor
DMEM	Dulbecco's modified eagle medium
EGFP	enhanced green fluorescent protein
F-actin	filamentous actin
INM	inner nuclear membrane
KASH	Klarsicht, ANC-1, Syne Homology
LAP	lamina-associated polypeptide
LBR	lamina B receptor
LEM	LAP2, emerin, MAN1
LINC	linker of nucleoskeleton and cytosceleton
NPC	nuclear pore complex
ONM	outer nuclear membrane
PAA	polyacrylamide
SUN	Sad1p, UNC-84

1. INTRODUCTION

When examining cells, the most prominent cell organelle is nucleus. Nucleus can be seen through cell surface as a bulge even when the cell is attached and spread over large area. Much of this property is thanks to its nuclear lamina, situated next to inner nuclear membrane (INM) and attached to it mainly via hydrophobic tail of lamin B protein and interactions with other transmembrane proteins of INM. The major components of the nuclear lamina are type V intermediate filament proteins called lamins. Nuclear lamins organize into a dense meshwork that gives structure and support for the nuclear envelope. Nuclear lamina serves as an attaching point for many intranuclear proteins, and especially for those taking part in chromatin organization, DNA replication, and gene expression. Lamins are therefore a major player in nuclear processes and help regulating many aspects of chromatin activity. Lamins have been indicated to be an integral part in overall nuclear dynamics by regulating the localization of nuclear pore complexes and the positioning of the nucleus itself inside the cell. It has also been shown that the nuclear lamina is coupled to the cytoskeleton via bridging proteins that span the nuclear envelope. This enables nuclear lamina to interact directly with cytoskeleton, through which it is in contact with the whole cell.

1.1. Nucleus and nuclear envelope

INM contains multiple different transmembrane and membrane bound proteins. Those located on the INM often interact with nuclear lamina and bridge it to the nuclear membrane. Most notable of these proteins are emerin, lamin B receptor, MAN1, and lamina-associated polypeptide-1 and -2 (LAP1 and LAP2). All of these proteins are targeted to INM and are not present in other parts of the cell. They also take part in lamina or chromatin binding to nuclear membrane (Gruenbaum et al., 2005). In addition, there are protein complexes that join cytoskeleton to nucleoskeleton, aptly named Linker of Nucleoskeleton and Cytoskeleton (LINC). Thus nuclear envelope protein collection is wide

and varying, with many proteins still poorly characterized and even new ones being found (Roux et al., 2012).

One of the most studied proteins of the nuclear lamina is lamin B receptor (LBR). It was found while studying lamin A and lamin B (Worman et al., 1988). Worman et al. detected that lamin B binds more effectively to nuclear envelope residues while lamin A showed significantly less binding. LBR differs from other mentioned transmembrane proteins by its tertiary structure and how it associates with nuclear membrane. LBR is a multi-pass transmembrane protein, containing eight transmembrane domains, while for example, MAN1 has only two and the other well known proteins have only one (Georgatos, 2001). LBR also contains two active binding sites in the hydrophilic N-terminus, that bind both lamin B and dual-stranded DNA (Olins et al., 2010). LBR also binds other membrane proteins and histones, and LBR is thought to regulate nuclear DNA distribution and gene expression (Solovei et al., 2013). However, LBR also forms a larger complex with LBR kinases, but exact functions of this complex are yet to be discovered.

Another important protein of the nuclear lamina is emerin, which associates with lamins and binds especially lamin A to INM (Bengtsson and Wilson, 2004). Together emerin and lamin A forms a complex which seems to be able to bind accessory proteins, especially barrier-to-autointegration factor (BAF) protein, which assists in chromatin binding and cell cycle regulation. BAF can bind emerin by its N-terminal LEM (LAP2, emerin, MAN1) domain that can also be found from MAN1 and LAP2. This might be the reason why these proteins have somewhat overlapping functions in chromatin binding and gene regulation. Emerin has also been shown to have an actin binding ability (Holaska et al., 2004). In their study Holaska et al. showed that purified emerin from nuclear extract had high affinity for binding to F-actin *in vitro*. The study suggests that actin binding properties of emerin have a significant part in organizing and stabilizing nuclear actin by binding to its pointed end.

LAP proteins are similar to emerin and consist of one transmembrane domain with lamin binding capability (excluding some nucleoplasmic LAP2 variants) and additional functional group at N-terminus. LAP1 proteins can bind both lamin A and lamin B, but associate mainly with B-type lamins *in situ* (Maison et al., 1997). LAP1 also binds to a yet unidentified protein kinase that phosphorylates nearby proteins, and can form larger

functional complexes with other INM proteins. LAP2 proteins on the other hand bind exclusively to lamin B and contain LEM domain for BAF binding as active region, similar to emerin (Shumaker et al., 2001). As with other LAM containing proteins, LAP2s are important chromatin binding mediators and promoters of replication.

MAN1 is a less well known INM protein, but still of great interest. Differing from other discussed proteins, it has two transmembrane domains, so that both C- and N-terminus are present inside the nucleoplasm. MAN1 is coded by the LEM domain-containing protein 3 (LEMD3) gene and as the name suggests, its main feature is an N-terminal LEM domain. MAN1 differs from emerin and LAP2 by its C-terminus, which can act as transforming growth factor TGF-β pathway regulator by binding SMAD proteins that antagonizes TGF signaling (Gruenbaum et al., 2005). Because of this property, MAN1 is also an important factor in embryo development.

As mentioned above, nuclear membrane also contains proteins to link together otherwise separate cytoskeleton and nucleoskeleton. Components of the so-called LINC-complex (linker of nucleoskeleton and cytoskeleton) are Sad1p, UNC-84 (SUN) and Klarsicht, ANC-1, Syne Homology (KASH) domain containing proteins (Chang et al., 2015). SUN proteins reside in INM and connect at the perinuclear space to KASH, which penetrates the outer nuclear membrane (ONM). SUN proteins form trimers together and their SUN domains in perinuclear space can bind up to three different KASH proteins (Tapley and Starr, 2013). Nucleoplasmic part of SUN proteins binds lamins with high efficiency and is also thought to bind other intranuclear and nuclear membrane proteins. KASH domain proteins are transmembrane proteins on the ONM that have ability to bind motor proteins or cytoskeletal components directly. This allows LINC complex to attach nucleus to cytoskeleton for nuclear movement, rotation and also for transmission of mechanical forces (mechanotransduction) (Chambliss et al., 2013).

1.2. Lamins

Lamins have been shown to be evolutionary the oldest intermediate-filament proteins in eukaryotic cells (Goldman et al., 2002). Two main types of lamin have been identified, A-type and B-type. B-type lamins are found in nuclear lamina at all times and they are the primary building block for the nuclear lamina. On the other hand, A-type lamins are more

mobile and can polymerize to nuclear lamina when more support is needed (Goldberg et al., 2008). Both lamin types are very conserved in metazoans, which already shows their importance for the cellular functions and normal physiology. Lamin A/C deficiency and mutations have been shown to cause nuclear instability, such as muscular dystrophy (Lammerding et al., 2004). However, cells can live without lamin A, but it is vital for higher organisms and differentiated tissues to function properly. On the other hand, it has been shown with depletion experiments, that lamin B is essential for normal nuclear formation, as cells without lamin B cannot form nuclear envelope or the nucleus is small and fragile (Tang et al., 2008). Depletion of lamin B also induces apoptosis of the cell.

General structure of lamins is similar to other intermediate filament proteins, an α-helical coiled coil dimer structure with a small globular C-terminus (Davidson and Lammerding, 2014). Differences are in the way lamin proteins are arranged into larger subunits. Polymerization is done in a head-to-tail fashion to form a strand of dimers that can then assemble into anti-parallel polymers. Lamins are distinguished by their biochemical properties, structural differences, and by their mobility in mitosis.

Lamin B has two main variations, B1 and B2, that are encoded by LMNB1 and LMNB2 genes. In addition to these, there is lamina B3 that is present in oocytes and is coded by LMNB2 gene. B-type lamins have slightly acidic isoelectric point and have a strong affinity to bind to nuclear membrane due to CaaX motif in the C-terminus (Stuurman et al., 1998). CaaX motif is a short amino acid sequence that features one cysteine, two aliphatic amino acids and random amino acid in the end. CaaX motif is usually found at the C-terminus of membrane-associated proteins. After translation, lamins containing the CaaX motif are post-translationally modified to have a hydrophobic tail for membrane association (Kitten and Nigg, 1991). Cysteine of CaaX motif undergoes isoprenylation in which 15- or 20-carbon long isoprenoid is attached to it (Gao et al., 2009). On top of this, aaX part is cleaved from the protein and C-terminus is methylated for more hydrophobic end. Because of these traits, lamin B is mainly bound to membrane and is free only during mitosis and only in low concentrations. Inner membrane of nuclear envelope also contains multiple membrane proteins that bind and interact with lamin B, most notable of these being lamin B receptor (LBR) (Gruenbaum et al., 2005).

Type-A lamins are encoded by single gene LMNA, which is spliced in different ways to get multiple different lamins. They are highly similar to lamin B, but have a neutral isoelectric point and their C-terminal CaaX motif is either cleaved off (lamin A) or is missing altogether (lamin C) (Stuurman et al., 1998). As CaaX motif is hydrophobic, it enhances the lamin B membrane binding ability but with lamin A, this hydrophobic end is cleaved away producing a neutral, soluble protein (Barrowman et al., 2008). This adds to dynamic property of lamin A and helps it to disassociate freely from nuclear lamina to nucleoplasm.

Different types of lamins polymerize into distinct networks, with their own proportions and shape, and still they affect each other while forming nuclear lamina (Shimi et al., 2015). B-type lamins are layered closely bound to inner membrane of the nucleus and form an even thin layer of filaments, and A-type lamins seem to build up on top of lamin B layer and form thicker filaments of variable length (Goldberg et al., 2008). A-type lamin layer also covers a wide area of nuclear lamina but seems to evade nuclear pore complexes. The distinct ways of polymerization of lamin types also indicate their different roles inside nucleus, B-type providing general structure for nucleus and lamina, and A-type acting as a dynamic reinforcing factor.

1.3. Actin

Actin is one of the main filament forming proteins of the cell. Actin takes part on a wide variety of cellular functions, for example as a component of the cytoskeleton and in cell motility. Although actin is mainly seen as a filamentous protein in cytosol, it also serves important functions inside the nucleus. Actin is not readily seen inside the nucleus because of its low concentration and inability to be labeled with conventional filamentous actin (F-actin) stains (Grosse and Vartiainen, 2013). Globular actin is also larger than the channel of the nuclear pore complexes (NPC), and so it does not readily diffuse passively into the nucleus (Stüven et al., 2003). This sieving effect is further enhanced by often used tagging of the actin by different fluorescent proteins, which increase the physical size of the tracked protein. However, when labeling actin monomers, actin inside nucleus can be detected in addition to cytoplasmic actin. This indicates that intranuclear actin is present in cells and actin is actively transported through NPCs. After actin was reliably detected

inside nucleus, more interest was aroused on its function and regulation. In the recent years it has become increasingly evident that actin is connected to almost every function inside nucleus (Miyamoto and Gurdon, 2013). These include transcription, chromatin and histone modification, and general assembly and localization of intranuclear components. After long debate, it was shown that actin can form filaments inside nucleus, and assemble into a loose network to maintain the nuclear organization (Plessner et al., 2015). Actin can also bind to emerin protein on the INM and therefore be connected to the nuclear lamina and even cytoskeleton via LINC-complexes (Holaska et al., 2004). With these various interactions, the whole cell is interconnected by an actin meshwork.

The most prominent and interesting aspect of nuclear actin is its part in gene regulation and genome modification. Studies indirectly suggest that actin and actin-related proteins (ARPs) may be integral part for the function of some RNA polymerases and they are localized to the same areas inside nucleus (Percipalle, 2013). Actin co-regulates the functions of RNA polymerase II by binding to it and serving as a binding point for other transcription factors (Hofmann et al., 2004). After initiating transcription, actin is hypothesized to be heavily present on elongation phase by recruiting histone modifying proteins, such as histone acetyltransferases, which are needed to keep the transcription ongoing (Obrdlik et al., 2008). As actin and ARPs can interact with chromatin remodeling complexes, they also take part on many nuclear processes, such as chromatin structural maintenance. Thus, actin seems to be an important mediator in nucleus, and one of the main questions is how it is regulated. Interesting aspect in this regard is the link between nuclear actin and the mechanical forces that a cell feels and is exposed to. As the whole actin network is connected from focal adhesion points to inside the nucleus, it is possible that intranuclear actin can be regulated by force (Plessner et al., 2015). This might be the case especially with nuclear F-actin. After reliable detection of F-actin inside nucleus became possible, it was shown that nuclear F-actin assembles upon cell spreading. Plessner et al. showed in their study that nuclear actin starts to polymerize when cells are spreading on a surface. After rapid actin polymerization inside nucleus, F-actin started to depolymerize. As cell spreading is mediated by integrin signaling, Plessner et al. also experimented with direct integrin activation by fibronectin. This activation produced similar results as cell spreading.

1.4. Mechanosensing and Polyacryl amide gels

In a living organism, tissue stiffness varies a great deal from brain to the bone (Wakatsuki et al., 2000), and cells have evolved to detect and alter their functions according to their surroundings. Cells react strongly to substrate elasticity measured by Young's elastic modulus (Yip et al., 2013). This modulus tells the ratio of stress to strain along an axis of force measured in pressure (Pascal) (Knight, 2008). The modulus indicates how much the object resists force before deforming elastically. For tissues, this modulus can range from under 1 kilopascal (kPa) of brain to over 30 kPa of bone (Tse and Engler, 2010). Depending on the location and function of the tissue, it needs to withstand many different kind of forces. As fibroblasts are the main cells of connective tissue, they naturally reside in a tense environment with stretching forces constantly applied to them (Wells, 2013). Other kind of forces to recon are shearing and pressure that some specialized cells are exposed to. For example osteoblasts and osteocytes from bone tissue react to amount of pressure and shearing exerted on them and function according to this pressure. Shearing force is also a factor with endothelial cells in the inner lining of blood vessels. Cells experience shearing force especially when fluids are flowing over them in high velocities relative to the cell.

Because cells need to work together and react to their surroundings, they must have an ability to sense the forces that are exerted on them. Therefore, cells have developed molecular assemblies for sensing those forces. Most notable and studied way of mechanosensing is related to focal adhesion points. As focal adhesions attach cells to their substrate, they have multiple different molecules that have an ability to react to forces mediated through them. One example is the talin protein that links focal adhesion integrin and vinculin to cytoskeleton. When force is applied to talin, its structure opens up and allows for vinculin binding with high-affinity (del Rio et al., 2009). This change therefore can initiate changes in the organization of cytoskeleton. As actin network spans the whole cell and connects adhesion points, it is no wonder that so many proteins are associated with mechanosensing. Luo et al. showed how different proteins of actin cytoskeleton were affected by different kind of forces. They found out that Myosin II reacted to tensional stress while filamin responded to shearing forces, providing better insight on direct effects of stress to cells (Luo et al., 2013). As mentioned above, cell nucleus is connected to the

adhesion points via actin cytoskeleton and LINC complexes. This enables forces to be transmitted directly to the nuclear envelope. Even though the details of the nuclear mechanosensing are still unclear, studies have shown that properties of the nucleus and gene expression can be altered by changes in the physical properties of the cell's surroundings.

As cells are subjected to such vast scale of forces in their natural environment, and have developed ways to sense and react to them, it is important to be able to study them in similar conditions. Polyacrylamide (PAA) is a polymer molecule composed of multiple acrylamide molecules. Acrylamide can be used to make hydrogels in conjugation with Bis-acrylamide acting as cross-linker. These gels are highly water-absorbent and can thus form soft gels for multiple uses. Hydrogels consist of interlinked polymer strands that are highly hydrophilic. Polymerized gel can absorb and retain high amount of water. In the field of molecular biology and biochemistry, they are mainly used in gel-electrophoresis experiments, but recently the usage of PAA gels have been more diverse as a simulation of different environmental stiffness for cells (Yeung et al., 2005). Advantages of PAA gels are their well established mechanical properties, easy tunability, and resistance to protein binding. PAA hydrogels provide one solution to mechanical manipulation of extracellular environment by providing an easily tunable stiffness, controlled by the acrylamide concentration and the amount of the cross-linker (Tse and Engler, 2010). These properties also offer the possibility to immobilize specific proteins to PAA gels, giving more control to the adhesion surface. This can be achieved by adding a chemical reagent that covalently links the protein to the PAA. With this addition, PAA-gels can be coated with proteins that allow cell adhesion, typically collagen or fibronectin.

2. AIMS OF THE STUDY

Main interest of this study was to investigate if mechanosensing can influence nuclear structures. Mechanosensing of the cells has been traditionally thought to happen at their adhesion points to surface (Seifert and Gräter, 2013). This however seems to be too restricted a view since the nuclear envelope is physically connected to the cell membrane via cytoskeleton (Chambliss et al., 2013). This mechanical connection links cell surface to

nuclear envelope that plays an important role on cell reacting to its surrounding environment (Lammerding et al., 2004). Actin forms stress fibers when cell is under higher tension and connects focal points to each other. When cells begin to attach to surface, an actin cap formed from actin fibers rapidly forms over the nucleus (Chambliss et al., 2013). The fibers of the actin cap connect the nucleus to the cellular adhesions. This connection can transduce forces from the actin network into the nucleus, and allows cell to rapidly feel and be directly in touch with its surroundings.

In order to understand how nuclear mechanotransduction can alter cellular functions, the influence of the extracellular substrate rigidity on lamin A and nuclear actin localization was studied by using different PAA-gels. We followed the nucleoplasmic pool of both of these proteins in two different PAA-gel rigidities. Similarly to lamins, actin has an important role in nuclear activities, which are still poorly characterized. It is however possible that actin polymerization into stress fibers might affect the amount of free intranuclear actin concentrations. This way, surrounding stiffness might affect the nucleus in a discrete way. This was studied by measuring actin levels of nucleus and cytosol in different substrate rigidities, and comparing the results.

3. MATERIALS AND METHODS

3.1. 3T3 cell cultivation

Cells used in experiments were mouse embryonic fibroblasts 3T3 cell-line. Cells used in control and spreading experiments were acquired from ongoing cell at passaging of 9 from Teemu Ihalainen. Cells used for all PAA-gel experiments were fresh thawed with passaging of 5. Cells were grown in 75 ml cell flasks with Dulbecco's modified eagle medium (DMEM) with 10% fetal bovine serum (FBS), 1% penicillium/streptomycin and 1% GlutaMax. Incubation was in +37 °C and 5% CO_2.

3.2. Cell transfection

Cells were transfected using Invitrogen Neon Transfection System, using the provided protocol and solutions from Invitrogen Neon 100 µl kit. Aim for one transfection was to

get 1.2 · 10^6 cells per reaction and 6 µg of DNA for 120 µl of cell suspension. Neon Transfection System's own protocol was followed closely with slight modifications. Cell suspension was made as 120 µl for easy of use and program for the machine was 1350 V, 2 pulses, 20 ms pulse length. After transfection cells were plated to 6-well culture plates with DMEM.

3.3. Multicolor immunolabeling of the cells

Excluding the control test, final samples always contained transfected EGFP-containing protein (either lamin A, emerin or actin), lamin B1 labeled with alexa 633, f-actin labeled with phalloidin, and DNA label as DAPI in mounting media. Basic immunolabeling protocol was used with Triton X-100 permaebilization buffer (0,5% BSA, 0,1% Triton X-100 in BPS). Firstly, cells were permaebilized for primary antibody (10 min, RT, ~1 ml permaebilization buffer). Primary antibody solution was added onto cells (50 µl rabbit anti-lamin B1, 1:500), and incubated (60 min, RT). Primary antibodies were washed away with permaebilization buffer, PBS, permaebilization buffer treatment (10 min each, RT). Secondary antibodies with label were pipetted onto cells (50 µl, anti rabbit-A633 1:200, and phalloidin-A555 1:100), and incubated (30 min, RT). Final wash was done with PBS (2x10 min, RT) and samples were mounted on microscope slides (Prolong-gold with DAPI).

3.4. PAA gel manufacture and stiffness controlling

First two gel experiments were done by protocol used in University of Tampere (derived from (Tse and Engler, 2010)). Since Tse and Engler had the mechanical properties of the gels well described, no further analysis was needed in that aspect. Gels were prepared on clean 18 mm * 18 mm coverslips. Coverslips were placed on a 80 °C hot plate. NaOH was added on the coverslip so that the entire glass was covered (400 µl) and left to dry. If NaOH layer was not uniform after drying, some water was added and left to dry again. When NaOH layer was uniform, 200 µl of aminosilane ((3-Aminopropyl)triethoxysilane, APTES) was added on the coverslip and incubated (200 µl, RT, 5 min). After incubation, coverslips were washed with water.

After washing APTES residues away, glutaraldehyde (200 µl, 0.5%) was added to give an even adhering surface for the gels. Glutaraldehyde was incubated (30 min, RT, under hood for airflow), washed away, and coverslips were left to dry over night. On these activated coverslips two different PAA-gels were produced with stiffness of ~1.5 kPa and another ~33 kPa (Table 1).

Table 1. **Recipes of gels used and their mechanical properties.**

	~1.5 kPa, 7% Acrylamide, 0.05% Bis	~33 kPa, 10% Acrylamide, 0.26% Bis
10x PBS	500 µl	500 µl
Acrylamide (40% stock)	940 µl	1250 µl
Bis (2% stock)	125 µl	650 µl
H_2O	3440 µl	2600 µl
Total Volume	5000 µl	5000 µl

After gel mixtures were mixed, they were degassed in a desiccator (10-15 min) to get rid of free oxygen that can interfere with polymerization. Activated coverslips were attached to the covers of a 6-well plate so that the coverslips were suspended over the well. Collagen was used to provide cells focal adhesion points in gel experiments. High quality 9 mm * 0.17 mm round coverslips were treated with collagen-I from rat tail solution (100 µl, 200 µg/ml in PBS) and let incubate under hood (1 h, RT).

After degassing, gel reaction was started with NHS-acetylic acid (5 µl, 10 mg/ml in DMSO), TEMED (10 µl), and APS (50 µl, 10% in PBS). After mixing quickly, enough gel was added to get a ~100 µm thick gel (6.4 µl of gel solution, $\pi * (4.5\ mm)^2 * 0.1\ mm \approx 6.4$ µl) on silane activated coverslips. After adding gel solution, one collagen treated coverslip was placed on top of the gel droplet and 6-well plate cover was put on the 6-well plate with some PBS for humidity. Gels were put into incubator to polymerize (37 °C, 1 h).

After polymerization, gels were submerged into PBS for a couple of minutes to loosen the round collagen-treated coverslip. Once gels had rested for a while, collagen coverslip was removed carefully with scalpel, and condition of the gels was checked. Gels were stored in 4 °C in PBS. First two gel batches were done in aforementioned way, but those gels had autofluorescence problems that affected imaging. With NaOH treatment, too much of APTES was attached to the surface and in the end, large amounts of

glutaraldehyde was left in the samples. When imaging, glutaraldehyde autofluorescence produced ambient light that disturbed signal from cells. The last gel batch was therefore done similarly as before, but without NaOH treatment to get rid of excess aminosilane and glutaraldehyde residues.

3.5. Control test on glass cover slips

Three different cell transfections were made for glass control. One with actin-EGFP, one with Lamin A-EGFP, and one with Emerin-EGFP. Cells were plated to 6-well plates with 0.17 mm precision coverslips activated with fibronectin (50 μg/ml in PBS, 1 h, RT) at the bottom. After incubation of ~16 h, cells were fixated with PFA (4%, in PBS, 10 min, RT). Five different labeling sets were made from fixated samples (Table 2).

Table 2. **Table of labeling used with control tests.** All the fluorophores were Alexa Fluor dyes of corresponding wavelength. Primary antibody dilutions used were 1:200 for lamin A, 1:100 for myosin II and 1:20 for lamin B1. Secundary antibody dilutions were 1:100 for phalloidin and 1:200 for all else. All dilutions were done in 3% PBS.

Sample	405 channel	488 channel	555 channel	633 channel
1.	DAPI	Actin-EGFP	Actin-Phalloidin	Lamin A
2.	DAPI	Emerin-EGFP	Actin-Phalloidin	Lamin A
3.	DAPI	Lamin A-EGFP	Actin-Phalloidin	Lamin A
4.	DAPI	Lamin B1	Actin-Phalloidin	Myosin II
5.	LaminA	Lamin B1	Actin-Phalloidin	Myosin II

Samples were imaged using LSM780 microscope system, with setting defined at microscope setup. Image analysis was done as depicted in image editing and analysis section.

3.6. Cell cultivation on gels and spreading test

A time related cell attachment test was done on glass coverslips with similar fibronectin coating as used on control test. Three different cell transfections were made, one for actin, emerin, and lamin A respectively. Transfected cells were incubated for two days (+37 °C , 5% CO_2) before transfer to treated coverslips. After transfer cells were incubated (+37 °C , 5% CO_2) in three time sets of 10 minutes, 2 hours and 24 hours, with one of each

transfection samples in each set. After incubation, each set was immediately fixated using PFA (4%, in PBS, 10 min, RT).

Gel experiments were conducted with two different transfections and two different gel stiffness. Lamin A and actin (labeled with EGFP) samples were plated directly on gels described before. Cells were incubated for 24 hours (+37 °C , 5% CO_2) before fixing. After fixing, samples were immunolabeled with the same protocol as before. On these samples, labels were DAPI at 405 nm, EGFP labeled protein at 455 nm, Actin-phalloidin at 555 nm, and lamin B1 at 633 nm.

3.7. Microscope and imaging setup

Microscope used for every experiment was Zeiss LSM 780 with Axio Observer microscope body. Used settings and hardware are listed in Table 3.

Table 3. **Used microscope objective and settings on all experiments.**

Objective	Plan-Apochromat 63x/1.40 Oil DICM27
Lasers	Diode 405, Argon 458, InTune 553, HeNe 633
Filters	MBS 488/633, f-MBS 405/550c
Detector set for	Alexa Fluor 405, 555, 488, 633
Nucleus stack setting	512x512, 4x zoom, 0.2 µm thick, pixel size 66 nm, 2x averaging
Whole cell image	Variable resolution and zoom, 0.2 µm thick, pixel size 65-70 nm, 2x averaging

3.8. Image editing and analysis

All the data from microscopy was deconvoluted with Huygens Essential software. Settings for the microscope were found automatically by the program. Pinhole back projection was calculated with SVI Back projected confocal pinhole calculator. Settings shown in Table 4 were used for all channels with output to 16 bit TIFF image.

Table 4. **Deconvolution settings used in Hyugens Essential.**

Alorithm	Classic MLE
PFS mode	Theoretical
Max Iterations	200
Iteration mode	Optimized
Quality chance thresh.	0.01%
S/N ratio	5
Background mode	Auto
Back. Estim. Rad	0.7
Relative background	0
Bleaching corr.	If possible
Brick mode	Auto

ImageJ2 was used for image analysis. With deconvoluted data, analysis was performed to get the projected areas (whole cell and nucleus) and intranuclear protein ratios for lamin A and actin. Intranuclear actin was compared to cytoplasmic actin by selecting a layer from cell image stack that had center of the nucleus visible. Mean intensity of 4 micron circular area was calculated with ImageJ ROI manager → measure → intensity tool. Values from inside the nucleus and from cytoplasm were measured and compared.

Colocalization was performed with ImageJ colocalization treshold tool, with scatter plot shown and all options enabled. Control test samples were used for colocalization test. For actin colocalization actin-EGFP and actin-phalloidin from Table 2 sample 1 were compared, and for lamin A sample 3 lamin A-EGFP was compared with Lamin A label. Before colocalization treshold a maximum intensity projection was made from each used channel and produced images were compared.

With lamin A, measurement intensity profile was measured from similar point of cell image stack. Intensity profile of a 20 pixels wide and 5 microns long line was measured so that the center of the line was at nuclear envelope. From intensity profile maximum value of lamina intensity was compared to the mean of a 1 micron long part of the line that was inside nucleus.

Area analysis pipeline consisted of taking a Z projection of stack with maximum intensity → gaussian blur with radius of 1.0 → treshold with Otsu method and dark

background to get black cell or nucleus → Binary fill holes to get even area → select area and measure for area data.

For statistical significance, a T-test was used to compare mean values between two groups. T-test gives result as a p-value that defines how probable it is that the difference in mean value is due to variance in the data groups. As a general rule, results of 0.05 and lower can be considered statistically significant, and the closer to zero the p-value is, the more likely the difference is real. The applied T-test was one-tailed test for samples with unequal variance.

4. RESULTS

4.1. Construction of PAA gels

Main method for these studies were rigidity tunable PAA gels, which were constructed in two different rigidities with Young's modulus of 1.5 kPa or 33 kPa. Protocol for gel manufacturing was based on well-established methods, that allowed easy control on gel properties (Tse and Engler, 2010). Theoretically gels were 100 μm thick after polymerization and would isolate cells from the tension of the glass surface. Stiffer 33 kPa gels were successful apart from a few broken coverslips during removal. There were more difficulties in the construction of 1.5 kPa gels, as they were less rigid. The collagen coated coverslip attached to the gel very tightly, and in many of the gels tore some of the gel with it when removed. Despite these difficulties, the gels used in the experiment were visually determined to be usable and to have a smooth and homogenous surface. After the first set of gels were analyzed, it was noticed that there was a lot of unspecific fluorescence. This seemed to be connected to aminosilane treated coverslip, as autofluorescence was highest under the gel. This problem was circumvented when NaOH was no longer used in the treatment of the coverslips. This produced the desired effect and no more unspecific labeling or autofluorescence was present.

4.2. Cell spreading experiments

Cell spreading tests with cell seeding time points of 10 minutes, 2 hours and 24 hours on glass were conducted to get reference data of cell spreading on “infinitely” hard surface (Figure 1). This test also served as a benchmark on how nuclear lamina bound lamin A and intranuclear actin ratios change during attachment to hard surface. Logically, the longer the cell is allowed to spread on a glass surface, the further it spreads, until a maximum spreading area is reached. Similar area evaluation was performed on cell nuclei to see how time and rigidity affects nucleus size (Table 6). Same area evaluation was done to cells on gels for comparison against cells on glass (Figure 2).

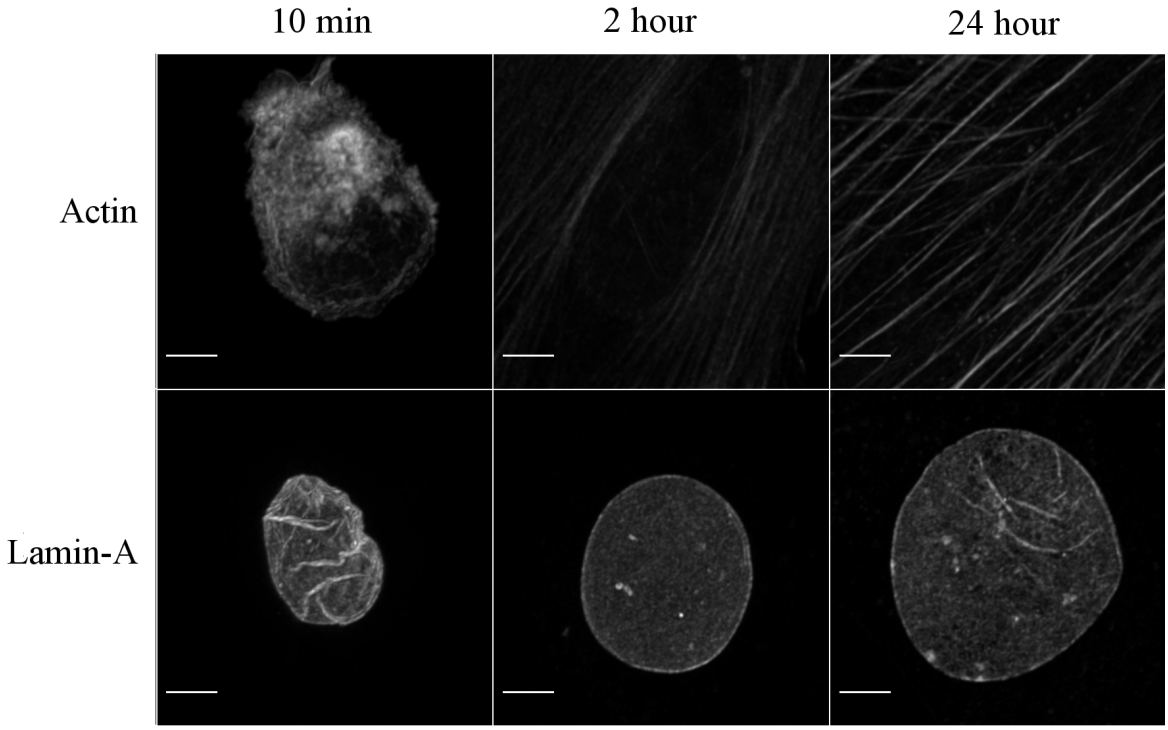

Figure 1. **Spreading experiment on glass.** Images taken from glass spreading experiment at corresponding time points. Both actin and lamin A show only area around the nucleus to show comparable effect of attachement time. Images are maximum intensity projections of image stacks with scalebar length of 5 µm.

In these experiments, cells on glass showed a cell spreading area similar to a normal yield curve with a fast initial increase in the spreading area, which slowed down in 24 hour sample being only about two times larger than 2 hour sample (Table 5). On the other hand, cells seeded on PAA gels spread at lower rate over the 24 hour incubation. Cells on the 1.5 kPa gel grew out to be about half of 2 hour sample's size and 33 kPa sample cells only little larger than the 2 hour sample.

Table 5. **Projected cell area data.** Data gathered from both lamin A and actin transfected cells were combined into one average value of cell size. Area calculated from z-projection of cell to get area that cells occupy.

	Cell area (μm^2)
10 min spreading	310 ± 30
2 h spreading	2400 ± 200
24 h spreading	4100 ± 500
1.5 kpa gel	1080 ± 110
33 kpa gel	3000 ± 300

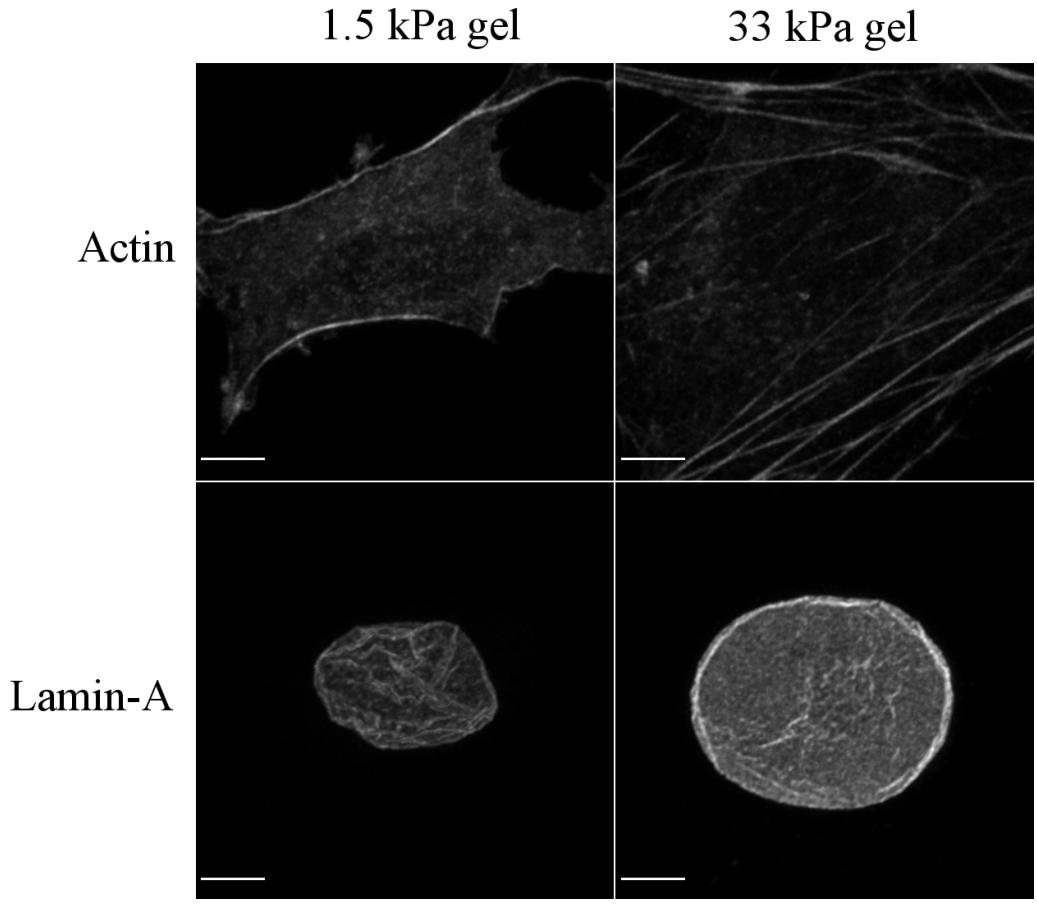

Figure 2. **Cell spreading on gels.** Image showing the effect of gel rigidity on cell and nucleus spreading. Images are maximum intensity projections of image stacks with scalebar length of 5 μm.

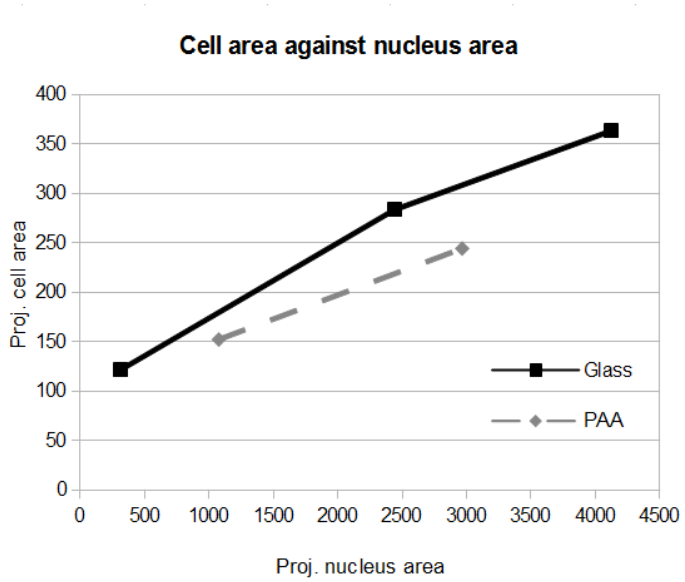

Figure 3:**Plot of projected cell area against projected area.** Seeding values include timepoints in order 10 minute, 2 hour, and 24 huor. For the gels, points are in order of 1,5 kPa and 33 kPa gel. Nucleus areas were calculated into a single total average value.

Cells grown on glass showed similar growth of the projected area of the nucleus as the whole cell, with declining speed of growth compared to growth time. Cells grown on gels on the other hand have considerably smaller projected area of the nuclei than cell size would lead to expect (Table 6, Figure 3). Cells cultivated on a 1.5 kPa gel have nuclei similar in size to 10 minute seeding time point on glass, and even cells on a 33 kPa gel have smaller nuclei than 2 hour cells. As can be seen on Table 6, lamin A-EGFP expressing cells have a consistently larger projected area of nucleus than those cells expressing actin-EGFP. When considering this difference statistically, the 2 hour sample has a clear difference, but at the 24 hour time point the difference has no real statistical relevance. Only at 10 minute spreading time point actin-EGFP nucleus size is larger than lamin A-EGFP, and this can be accounted to the fact that the nucleus is more folded and rounded when a cell is not yet attached to surface, and projected area is inaccurate even though T-test shows significant difference in values. This was seen as a large deviation in the sizes of individual nuclei compared to each other. With larger sample sizes, accuracy of measurements would be higher.

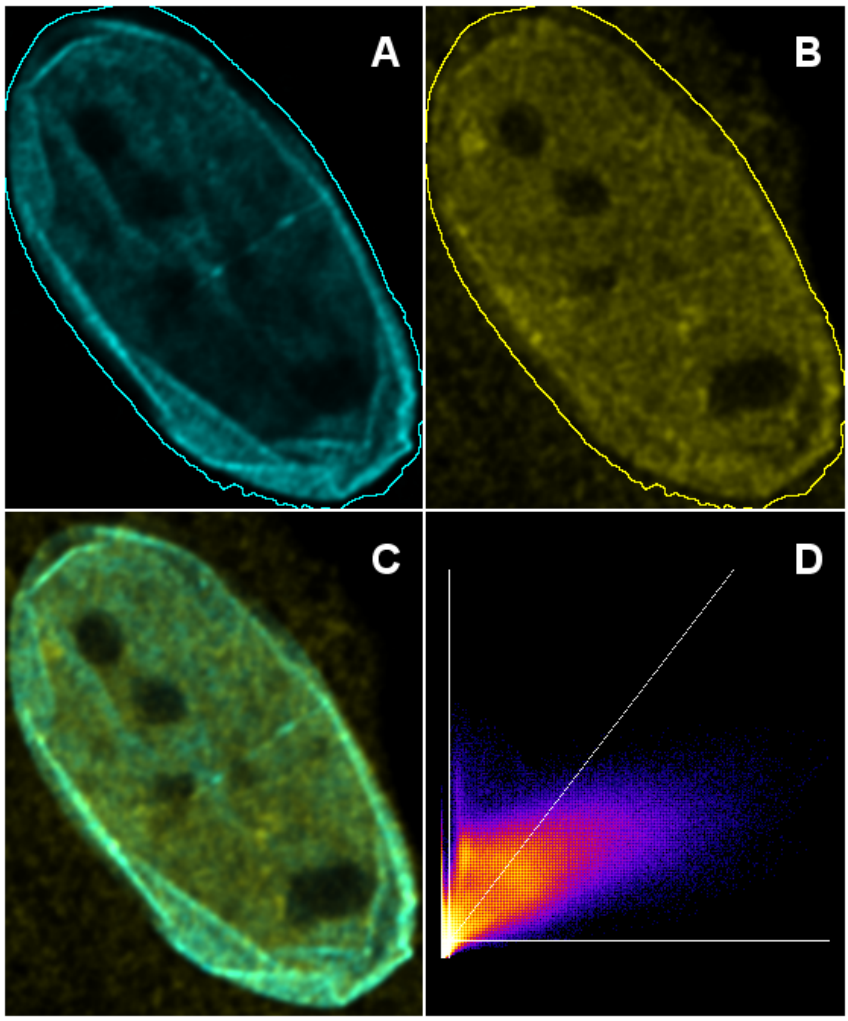

Figure 4. **Colocalization of lamin A-EGFP with immunolabeled lamin A/C.** Colocalization was performed to see if EGFP-tagged lamin A localizes as intended. Panel A shows lamin A-EGFP label, B shows immunolabeled lamin A/C, C shows merge image of both channels. Panel D shows a scatter plot with lamin A-EGFP channel as x-axis and lamin A/C channel as y-axis. Lamin A/C had a fair amount of unspecific fluorescence that tilts linear regression fit with a slope of m = 1.31.

Table 6. **Projected nucleus area data.** Average nucleus area values were calculated similarly as projected whole cell area, but lamin A and actin transfections values were kept separate to see if more expressed lamin A affects the size of the nucleus.

	Lamin A nucleus area (μm^2)	Actin nucleus area (μm^2)	T-test comparison, p-value
10 min spreading	110 ± 8	130 ± 10	0.031
2 h spreading	320 ± 30	250 ± 14	0.005
24 h spreading	380 ± 30	350 ± 30	0.200
1.5 kpa gel	170 ± 20	130 ± 20	0.058
33 kpa gel	270 ± 20	222 ± 14	0.024

4.3. Localization of lamin A

Lamin A-EGFP transfection was successful, and high yield of cells expressed it. Colocalization analysis of lamin A-EGFP with lamin A/C staining gave values of 0.87 for pearson coefficient, 1 for Mander's coefficient for lamin A-EGFP channel, and 0.69 for

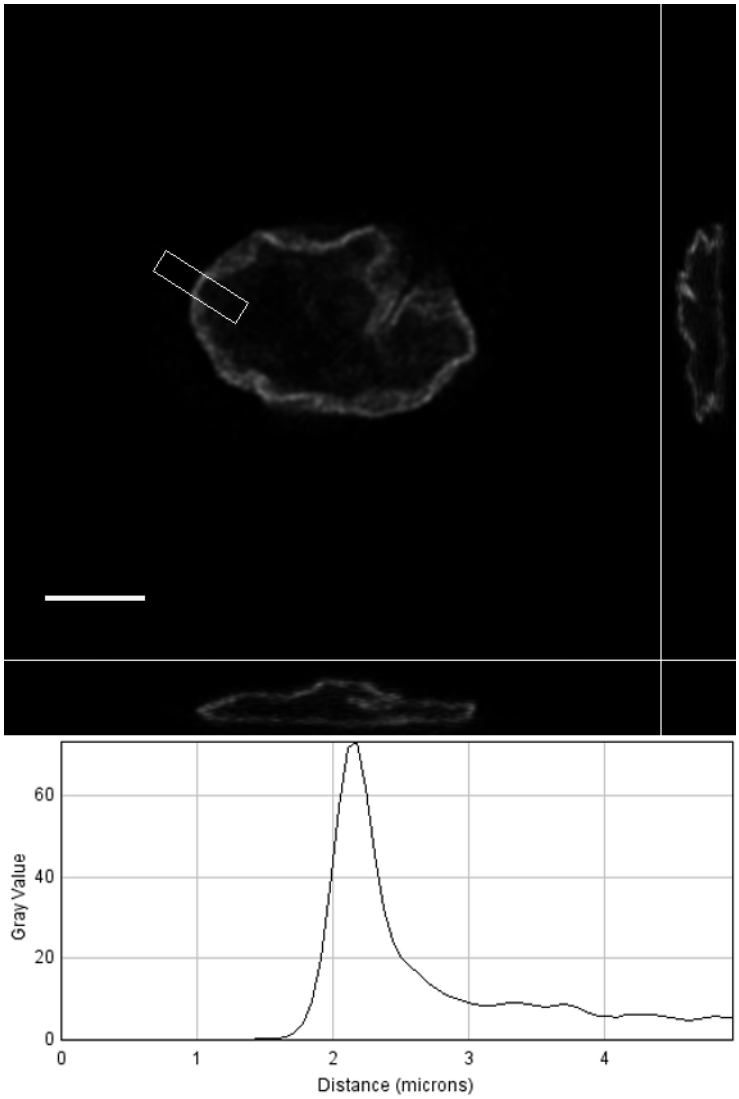

Figure 5. **Measurement of lamin A-EGFP intensity plot.** Panels with orthogonal view of a cells nucleus showing lamin A-EGFP and an intensity profile measured from area defined with borders. Intensity profile was used to find a maximum intensity value from the nuclear envelope and a mean intensity value from inside the nucleus by calculating an average intensity from last 1 µm of the profile. Scalebar length 5 µm. The cell in the figure was cultivated on a 1.5 kPa gel.

Mander's coefficient for lamin A/C channel. Merge image (Figure 4C) of those channels shows direct overlap on intensity and place on multiple areas. Scatter plot of pixel intensities from these channels is askew, because of background on lamin A/C antibody channel (Figure 4D). The plot still shows a general direction with linear regression slope of 1.31, still close to 1.5 of full colocalization.

Ratio of free lamin A compared to membrane-bound was calculated by measuring an intensity line profile (Figure 5). The ratio between nuclear lamina and nucleoplasmic lamin

A was calculated by taking the average intensity of last micrometer from the intensity profile (to get intranuclear mean intensity) and the peak value from nuclear envelope. These ratios can then be calculated into an average value of bound versus unbound lamin A (Table 7).

In spreading experiments, nucleoplasmic lamin A intensity was considerably lower at 10 minute time point compared to later time points. Cells that had spread for 10 minutes had 27.5 times higher amount of lamin A bound to nuclear envelope compared to free nuclear lamin A. Comparatively at 2 and 24 hour time points the amount of nuclear lamina bound lamin A was only about 7 times higher than free nucleoplasmic lamin A. The 24 hour sample had a nearly identical ratio as the a 2 hour sample. Similar trend can be seen in 1.5 kPa gel samples, with nuclear envelope having 10 times higher intensity in the nuclear lamina and thus lamin A amount when compared to free internuclear lamin A. However, 33 kPa samples had only 5 times more bound lamin A, similarly to 2 and 24 hour spreading experiments. When comparing statistical difference between the seeding experiment results, 10 minute seeding against both 2 hour and 24 hour seeding data gives a p-value of 0.004. This means high statistical difference between the results. However, when comparing 2 hour to 24 hour, p-value is around 0.47, meaning statistically really low difference as half of the results can be accounted inside variance in measurement. P-value for 1.5 kPa and 33 kPa gel is 0.048, which is within the 0.050 limit of reliability.

Table 7. **Relation value of lamin A.** Values calulated by dividing the highest intensity gained from nuclear lamina with the mean intensity from 3 or 4 μm area inside nucleus.

	Nuclear lamina / Nucleoplasm
Control glass	3.2 ± 0.2
10 min seeding	28 ± 7
2 h seeding	7.06 ± 0.03
24 h seeding	7 ± 2
1.5 kpa gel	10 ± 3
33 kpa gel	5 ± 2

4.4. Dynamics of nuclear actin

Actin-EGFP transfection also succeeded, and when compared to phalloidin labeling it displayed a similar localization of stress fibers. Unlike phalloidin, actin-EGFP shows both

polymerized and monomeric actin, and is therefore a good tool to study intranuclear actin. However, this does not affect colocalization results, because intensity of free actin is so low that it is eliminated by the thresholding in the colocalization calculations. Colocalization values for actin were 0.84 for pearson coefficient, 1 for Mander's coefficient for lamin A-EGFP channel, and 0.99 for Mander's coefficient for lamin A/C channel. Colocalization comparison visually is more reliable with actin experiment. Merge image of Figure 6C shows clear overlap on cell area, especially at stress fibers. Scatter plot is also more linear and one to one with intensity values.

Actin ratio was calculated by dividing the mean value of a 3 micrometer wide area

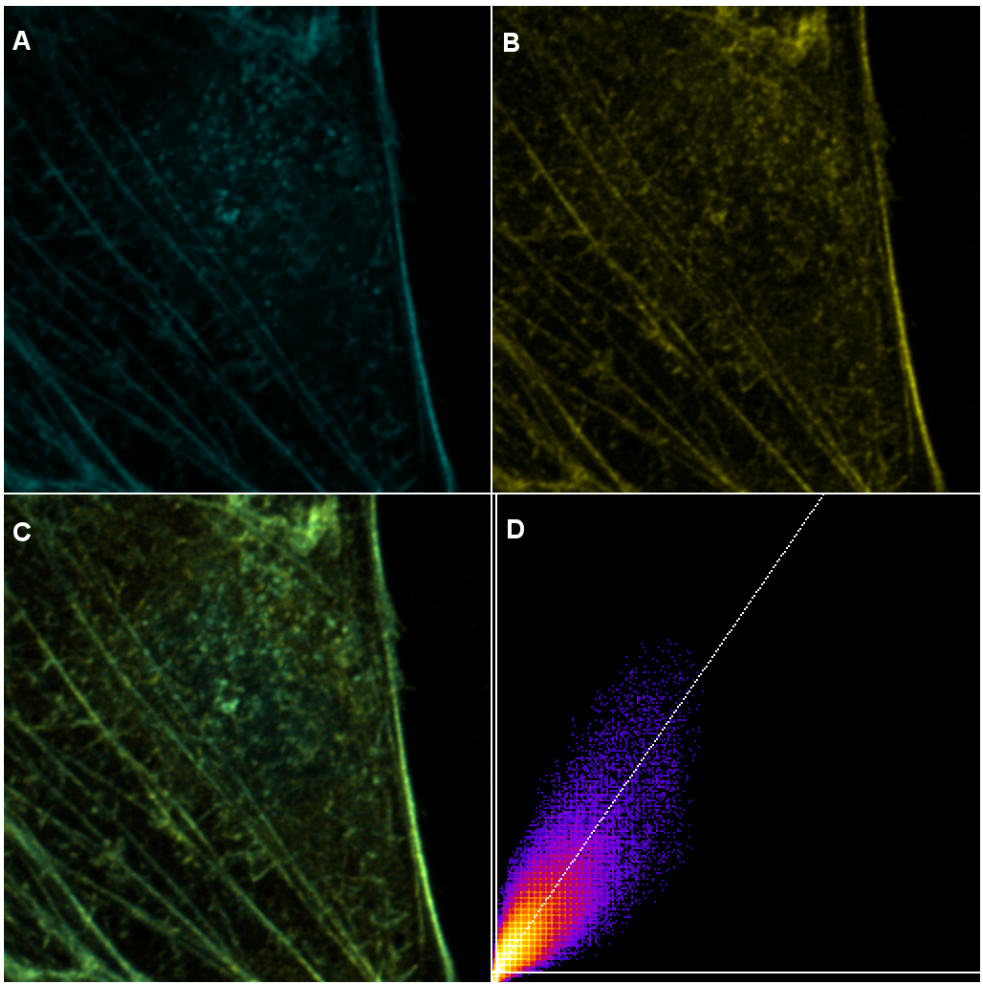

Figure 6. **Colocalization of actin-EGFP and phalloidin labeled actin.** Panel A shows cell expressing actin-EGFP, B shows phalloidin-Alexa Fluor labeled actin and C panel shows merge of these channels. Panel D shows a scatter plot with actin-EGFP as x-axis and phalloidin-alexa channel as y-axis. The scatter plot shows a good correlation between channels, and linear regression gives a slope of m = 1.46.

inside nucleus with similarly measured mean value from cytosol as shown in Figure 6. This

gives a relation for intranuclear and cytosolic actin that can be compared between the samples (Figure 7). Actin data from spreading experiment shows very slight decrease in ratio when cells have adhered to glass surface for longer time (Table 8). As the ratio is obtained by dividing nuclear actin signal by cytoplasmic, lower ratio would mean that relative nuclear actin amount is also lower. Differences in ratios are so small that they are within error limits, and p-value tested for data sets were over 0.4. This implies that most of the difference seen is statistically insignificant. Gel experiments on the other hand show a 75% increase in nucleoplasmic actin when cells were grown on stiffer gels, with standard error remaining about the same. P-value of 0.001 for actin gel comparison suggests that the difference is prominent. These results are similar to lamin A measurements.

Table 8. **Relation values of actin.** Values were calculated by dividing the mean intensity of a circular area with a diameter of 3 or 4 μm inside nucleus with a similiar area from cytosol.

	Actin Nuclear/Cytosol
Control glass	0.4 ± 0.6
10 min spreading	0.15 ± 0.04
2 h spreading	0.15 ± 0.02
24 h spreading	0.14 ± 0.03
1.5 kpa gel	0.26 ± 0.04
33 kpa gel	0.45 ± 0.04

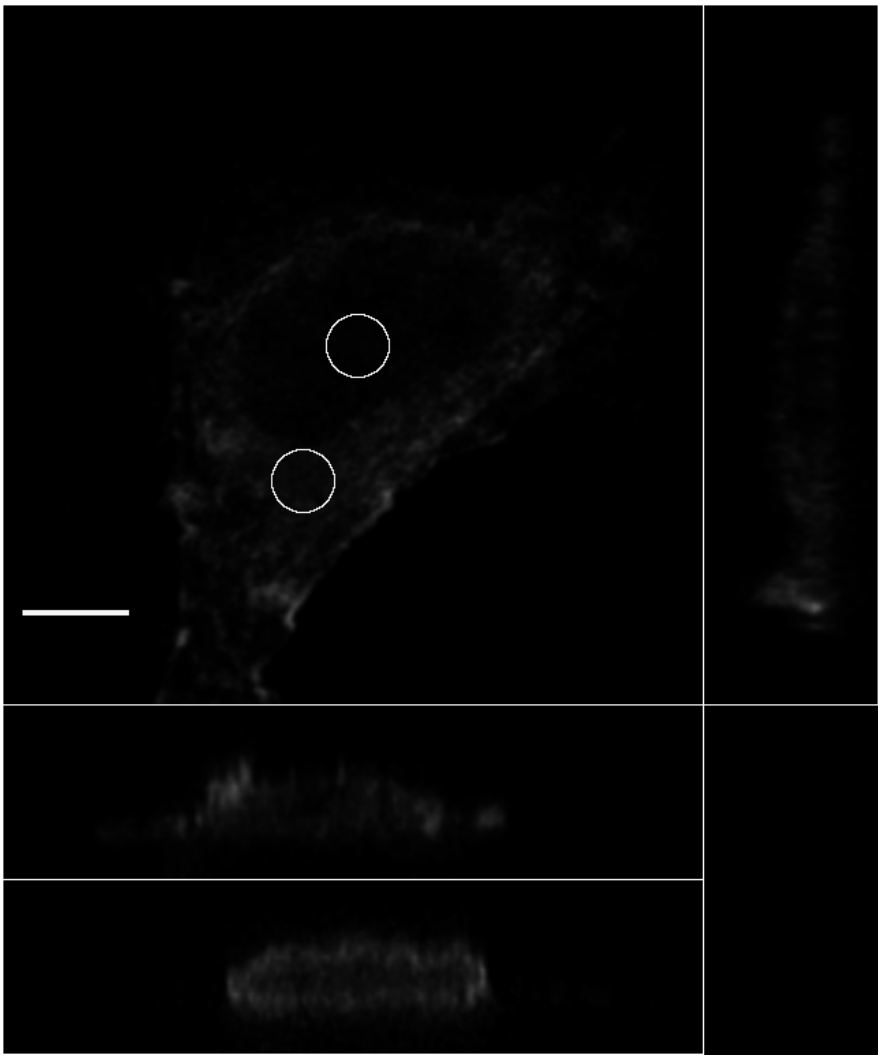

Figure 7. **Actin intensity ratio measurement.** Figure shows an orthogonal view of a cell expressing actin-EGFP with regions of interest for measuring mean intensity from inside nucleus and cytosol. These values were used to create final comparable results. Panel on the bottom shows same cell's nucleus with immunolabeled lamin B. Scale bar length 5 μm.

5. DISCUSSION

Nucleus of the cell is connected to cell membrane through complex interactions with cytoskeleton, nucleoskeleton and many proteins interlinking them. It has also been shown that a cell can transmit forces to nucleus and it is shown that some form of mechanosensing is also happening at nuclear lamina (Lammerding et al., 2004 and Swift et al., 2013). This mechanosensing is partly the reason why cells react to forces and substrate properties differently. This work focused on how substrate rigidity can alter lamin A and actin dynamics inside nucleus, and expands on the existing knowledge of how cell react to extracellular forces.

Initially emerin was considered as an additional protein to study, but cells transfected with emerin-EGFP construct showed abnormal emerin buildups. This might be due to EGFP label causing a change in protein-protein interactions and disturbing normal binding at the nuclear membrane. Additional emerin expression could hamper normal emerin transport and/or localization and cause aggregates when protein concentration is too high. As results with emerin proved to be unreliable, it was left out from the work. Still, lamin A and actin showed promise in preliminary tests, localizing as they should while cell vitality remained good.

5.1. PAA gels

In technical aspect, gels proved to be valuable tools with easily adjustable mechanical properties. Still, in course of the experiment, some serious problems arose. First difficulty came with NaOH activation of the primary coverslips. Method for applying uniformal NaOH surface and applying APTES over it left large quantities of APTES residues behind after washing. This residual APTES bound high amounts of glutaraldehyde, which produced autofluorescence and degraded image quality. This problem was circumvented by leaving out NaOH treatment of the coverslips and applying APTES straight to glass. APTES, glutaraldehyde, and gels all adhered well to glass surface and the quality of final images was better than before. Another difficulty was encountered when removing

collagen coated coverslip from 1.5 kPa gels surface. The glass bound to the gel so tightly that almost every gel broke apart, especially from the center region. This was not evident when checking gels before plating cells on them, but was seen on microscope as cells could not adhere or spread properly in the middle. Cells from these gels were finally imaged closer to the edge of the gel. Edge of the gel might have been dryer than that at the center and so stiffer than the expected 1.5 kPa. This might have some effect on measurements, but difference between used gels was still considerable. This problem could be circumvented by using a primary protein coating on the coverslips before collagen coating. This would allow collagen to detach from the glass more easily and allow better quality gels.

5.2. Cell and nuclear spreading

This experiment revolved around a method that allows cells to grow on more natural and tunable surface. Tunability of PAA-gels is centered in stiffness manipulation as in this experiment, but different protein coating can also be attached to gel surface for cells to adhere to. Microscopic experiments normally involve cells seeded directly on a glass surface, which is by cellular standards an infinitely hard surface. This causes cells to adhere tightly, spread efficiently, and form an extensive cytoskeleton with pronounced stress fibers. As mentioned before, cells are affected by the stiffness of the extracellular environment, and PAA gel surface gives control on the rigidity of their surroundings. In this experiment, gels were used to simulate two surfaces with different rigidity, gels with Young's modulus of 1.5 kPa and 33 kPa. Effect of the rigidity can be seen in cell spreading area that indicates how well cells can attach to the surface and spread. On the glass surface cell spreading experiment, effect of a hard surface can be readily seen. Cells attach easily to a hard surface and can spread rapidly over larger surface area than on a softer matrix. Cells also react to a hard surface by forming actin stress fibers to support the spreading. When cells first attach to glass for 10 minutes, they are more globular than flat. As time progresses to 2 hour mark, cells have gained over seven times the surface area and stress fibers have grown more substantial, as seen in Figure 1. This spreading carries out steadily, so that 24 hour sample shows still almost two fold increase in surface area compared to 2 hour sample. On the other hand, cells on gels did not spread as drastically. Softer 1.5 kPa

gel cells showed mean cell spreading area smaller than that of 2 hour on glass, and 33 kPa gel cells grew out only just larger cell surface area than 2 hour sample. Some of this effect can also be accounted to a denser protein coating for the cells to attach to. When coating glass surface with protein, it retains a smooth surface, but gels are a meshwork with less area for the proteins to attach to. Still, this firmly shows that surface stiffness has an effect on these cells morphologically.

The projected area of the nucleus shows similar behavior as cell spreading area, with projected nucleus area increasing on stiffer gel. This result is consistent with findings of Lovett et al. (2016) that showed size of the cell to be linked to the height of the nucleus, and vice versa. When loosely attached, the nucleus is fairly globular and small when measured directly from above. Nucleus is also often wrinkly, decreasing the projected surface area of the nucleus. This might be due to cell not having enough adhesion points with surface and being yet unable to form an actin cap over the nucleus to flatten it. However, nuclei of the cells grown on gels did not spread as far as expected on the basis of cell spreading area data, and both are below the area of the 2 hour seeding tests cells (Figure 3). In the end, both cell and nucleus size of cells grown on 33 kPa gel were 40% smaller than those grown on glass. Cells grown on stiffer gel had 50% larger nucleus than those grown on softer gels. This size difference arises from cell maintaining nucleus size in relation to cell size and from how flat the nucleus is. When grown on a more rigid environment, cell nucleus also spreads and flattens out (Lovett et al., 2013). Another difference can be seen between lamin A and actin transfected cell nuclei. At all other time points than 10 minute, lamin A transfected cells had larger nuclei. This could be due to additional lamin A produced from transfected gene. As lamin A is a supporting component of nuclear lamina and has an important part on governing the shape of the nucleus, this additional lamin A might give nucleus more support and keep it flatter. However, comparison of 24 hour seeding results is statistically insignificant in this sense and comparison of 1.5 kPa gel samples gives a p-value only slightly over the 0.05 limit. Some of this can be accounted to a small sample size, as omitting the largest value from 1.5 kPa samples results in a p-value close to 0.02, meaning a more significant difference. These results are therefore only approximates, as sample size was between 10 and 15. Good

reliability would usually need around 30 samples depending on variance in the data set. Still, similar regular difference was not measurable in whole cell size measurements.

5.3. Lamin A localization

Colocalization of expressed lamin A-EGFP with immunolabeled lamin A/C showed that used construct localized correctly to nuclear lamina. Pearson's correlation coefficient for these channels is 0.87, indicating that colocalization is fairly high as 1 means perfect colocalization. In addition to this, Mander's coefficient for lamin A channel is 1 showing that all pixels over treshold are localized with pixel from lamin A/C channel. Mander's coefficient for lamin A/C channel is 0.69 because of quite large amount of non specific labeling visible on Figure 4 and scatter plot. These results however show that lamin A-EGFP is reliably targeted to nuclear membrane.

Lamin A measurements showed constant increase in free nuclear lamin A during the cell seeding and in more rigid gels. For cells grown on glass for 2 and 24 hours, the ratio between nucleoplasmic and nuclear lamina bound lamin A is almost 4 times smaller than those seeded for 10 minutes. This would indicate that when cells gain foothold and start to spread, the amount of free lamin A in the nucleoplasm increases. Gel experiment shows similar results with 33 kPa gel having 2 times lower lamin A ratio than 1.5 kPa gel. As before, this means that free intranuclear lamin A is more abundant in cells growing on stiffer surface. Even though it has been shown that lamin A is phosphorylated (Buxboim et al., 2014), and more mobile when cells are in less stiff environment, it is possible that results show net increase of lamin A expression. This is backed by a study that showed lamin A levels to increase with stiffer environment (Swift et al., 2013), reinforcing the nucleus when needed.

5.4. Actin dynamics

Actin-EGFP construct's localization was also verified by comparing it with phalloidin-labeled actin cytoskeleton. Pearson's coefficient for these channels was 0.84 and still high enough to be considered good colocalization. Mander's coefficients showed better result with coefficient of actin-EGFP channel of 1 and actin-phalloidin channel of 0.99. This signifies that almost all of the pixels colocalize on both channels. Better Mander's

coefficient for actin than for lamin A label is partly because actin fibers give higher intensity result. Phalloidin was also tagged with a fluorophore that had a lower emission wavelength, which gives a greater resolution compared to anti-lamin A label.

Actin's dynamics proved to be more difficult with glass seeding test showing only slightly lower amount of nuclear actin compared to cytosolic actin. Glass seeding test results had a slightly lower ratio as cells attach more firmly to glass than to gel. This would indicate that less actin is needed inside nucleus after attachment. However, as results are all very close to each other, almost within error limit, and p-value from comparisons is over 0.4 on all accounts, this conclusion is not reliable. Another possibility is that actin amount inside nucleus does not change that rapidly. As this experiment included cell trypsination and seeding within only short period of time, it might be that nuclear actin levels did not have enough time to respond. When cells are trypsinated, they end up in different environment within 5 to 10 minutes, and normally large scale cell movement and changes in structure happen relatively slow, in tens of minutes and multiple hours in case of cell attachment to substrate (Li et al., 2014). However, results from gel experiments show clear difference with 33 kPa gel actin ratio being 75% larger than that of the 1.5 kPa gel. This indicates that when cells are grown on more rigid surface and sense higher forces, they transport more actin into the nucleus. It has also been shown that actin transport into the nucleus is increased when cells are put under stress (Johnson et al., 2013). In this light, it seems that actin is actively transported in greater quantities into to nucleus the harder the surface is.

5.5. Error sources of the experiments and future prospects

The main error source in the experiment is the bleedthrough of fluorescence from different optical planes to the center of the nucleus, thus the cytoplasmic fluorescence can be detected also inside the nucleus. This is also more pronounced on flatter nucleus and especially in actin measurements. When cells form thick stress fibers that contain same EGFP labeled actin, they become extremely strong fluorescence emitters. For this reason, it is difficult to find a level with no background fluorescence from the center of the nucleus. The same happens with lamin A, as nuclear lamina is strongly fluorescent and in flat nucleus bleedthrough from upper and lower layers is noticeable.

In future experiments, this method should be used first to gather more data on multiple different PAA gel rigidities. With intermediate and more rigid surface added to these results, a trend curve could be plotted to show how the surface really affects intranuclear amount of lamin A and actin. Also, actin associated proteins and proteins that have a connection to lamin A should be included, mainly emerin and nuclear myosin I. Emerin is an important factor in connecting nuclear lamina to the nuclear envelope and assisting membrane anchorage with LINC complex. Studying emerin dynamics would give insight of its part in force transit and detection. Nuclear myosin I has an emerging role on activities with nuclear actin. Myosin has been found to be an important activator on transcription initiation (Hofmann et al., 2006), providing even more evidence on the importance of actin and actin associated proteins inside nucleus. Intranuclear myosin studied in association with actin would provide information on what is needed for nucleus to manage its components in different conditions.

6. REFERENCES

Barrowman, J., C. Hamblet, C.M. George, and S. Michaelis. 2008. Analysis of prelamin A biogenesis reveals the nucleus to be a CaaX processing compartment. *Mol. Biol. Cell*. 19:5398–5408. doi:10.1091/mbc.E08-07-0704.

Bengtsson, L., and K.L. Wilson. 2004. Multiple and surprising new functions for emerin, a nuclear membrane protein. *Curr. Opin. Cell Biol.* 16:73–79. doi:10.1016/j.ceb.2003.11.012.

Buxboim, A., J. Swift, J. Irianto, K.R. Spinler, P.C.D.P. Dingal, A. Athirasala, Y.R. Kao, S. Cho, T. Harada, J.W. Shin, and D.E. Discher. 2014. Matrix Elasticity Regulates Lamin-A,C Phosphorylation and Turnover with Feedback to Actomyosin. *Curr. Biol.* 1909–1917. doi:10.1016/j.cub.2014.07.001.

Chambliss, A.B., S.B. Khatau, N. Erdenberger, D.K. Robinson, D. Hodzic, G.D. Longmore, and D. Wirtz. 2013. The LINC-anchored actin cap connects the extracellular milieu to the nucleus for ultrafast mechanotransduction. *Sci. Rep.* 3:1087. doi:10.1038/srep01087.

Chang, W., H.J. Worman, and G.G. Gundersen. 2015. Accessorizing and anchoring the LINC complex for multifunctionality. 208:11–22. doi:10.1083/jcb.201409047.

Davidson, P.M., and J. Lammerding. 2014. Broken nuclei - lamins, nuclear mechanics, and disease. *Trends Cell Biol.* 24:247–256. doi:10.1016/j.tcb.2013.11.004.

Gao, J., J. Liao, and G.Y. Yang. 2009. CAAX-box protein, prenylation process and carcinogenesis. *Am. J. Transl. Res.* 1:312–325.

Georgatos, S.D. 2001. New embo member's review: The inner nuclear membrane: Simple, or very complex? *EMBO J.* 20:2989–2994. doi:10.1093/emboj/20.12.2989.

Goldberg, M.W., I. Huttenlauch, C.J. Hutchison, and R. Stick. 2008. Filaments made from A- and B-type lamins differ in structure and organization. *J. Cell Sci.* 121:215–225. doi:10.1242/jcs.022020.

Goldman, R.D., Y. Gruenbaum, R.D. Moir, D.K. Shumaker, and T.P. Spann. 2002. Nuclear lamins : building blocks of nuclear architecture. 533–547. doi:10.1101/gad.960502.

Grosse, R., and M.K. Vartiainen. 2013. To be or not to be assembled: progressing into nuclear actin filaments. *Nat. Rev. Mol. Cell Biol.* 14:693–7. doi:10.1038/nrm3681.

Gruenbaum, Y., A. Margalit, R.D. Goldman, D.K. Shumaker, and K.L. Wilson. 2005. The nuclear lamina comes of age. *Nat. Rev. Mol. Cell Biol.* 6:21–31. doi:10.1038/nrm1550.

Hofmann, W. a, L. Stojiljkovic, B. Fuchsova, G.M. Vargas, E. Mavrommatis, V. Philimonenko, K. Kysela, J. a Goodrich, J.L. Lessard, T.J. Hope, P. Hozak, and P. de Lanerolle. 2004. Actin is part of pre-initiation complexes and is necessary for transcription by RNA polymerase II. *Nat. Cell Biol.* 6:1094–1101. doi:10.1038/ncb1182.

Hofmann, W. a, G.M. Vargas, R. Ramchandran, L. Stojiljkovic, J. a Goodrich, and P. de Lanerolle. 2006. Nuclear myosin I is necessary for the formation of the first phosphodiester bond during transcription initiation by RNA polymerase II. *J. Cell. Biochem.* 99:1001–1009. doi:10.1002/jcb.21035.

Holaska, J.M., A.K. Kowalski, and K.L. Wilson. 2004. Emerin caps the pointed end of actin filaments: Evidence for an actin cortical network at the nuclear inner membrane. *PLoS Biol.* 2.

doi:10.1371/journal.pbio.0020231.

Johnson, M. a., M. Sharma, M.T.S. Mok, and B.R. Henderson. 2013. Stimulation of in vivo nuclear transport dynamics of actin and its co-factors IQGAP1 and Rac1 in response to DNA replication stress. *Biochim. Biophys. Acta - Mol. Cell Res.* 1833:2334–2347. doi:10.1016/j.bbamcr.2013.06.002.

Kitten, G.T., and E. a. Nigg. 1991. The CaaX motif is required for isoprenylation, carboxyl methylation, and nuclear membrane association of lamin B2. *J. Cell Biol.* 113:13–23. doi:10.1083/jcb.113.1.13.

Knight, R.D. 2008. Physics for Scientists & Engineers: A Strategic Approach Plus Modern Physics. 580.

Lammerding, J., P.C. Schulze, T. Takahashi, S. Kozlov, T. Sullivan, R.D. Kamm, C.L. Stewart, and R.T. Lee. 2004. Lamin A / C deficiency causes Tema Grupo defective nuclear mechanics and mechanotransduction. *J. Clin. Invest.* 113:370–378. doi:10.1172/JCI200419670.Introduction.

Li, J., D. Han, and Y.-P. Zhao. 2014. Kinetic behaviour of the cells touching substrate: the interfacial stiffness guides cell spreading. *Sci. Rep.* 4:3910. doi:10.1038/srep03910.

Lovett, D.B., N. Shekhar, J.A. Nickerson, K.J. Roux, and T.P. Lele. 2013. Modulation of Nuclear Shape by Substrate Rigidity. *Cell. Mol. Bioeng.* 6:230–238. doi:10.1007/s12195-013-0270-2.

Luo, T., K. Mohan, P.A. Iglesias, and D.N. Robinson. 2013. Molecular mechanisms of cellular mechanosensing. *Nat. Mater.* 12:1064–71. doi:10.1038/nmat3772.

Maison, C., A. Pyrpasopoulou, P. a. Theodoropoulos, and S.D. Georgatos. 1997. The inner nuclear membrane protein LAP1 forms a native complex with B-type lamins and partitions with spindle-associated mitotic vesicles. *EMBO J.* 16:4839–4850. doi:10.1093/emboj/16.16.4839.

Miyamoto, K., and J.B. Gurdon. 2013. Transcriptional regulation and nuclear reprogramming: Roles of nuclear actin and actin-binding proteins. *Cell. Mol. Life Sci.* 70:3289–3302. doi:10.1007/s00018-012-1235-7.

Obrdlik, A., A. Kukalev, E. Louvet, A.-K.O. Farrants, L. Caputo, and P. Percipalle. 2008. The histone acetyltransferase PCAF associates with actin and hnRNP U for RNA polymerase II transcription. *Mol. Cell. Biol.* 28:6342–6357. doi:10.1128/MCB.00766-08.

Olins, A.L., G. Rhodes, D.B.M. Welch, M. Zwerger, and D.E. Olins. 2010. Lamin B receptor: multi-tasking at the nuclear envelope. *Nucleus*. 1:53–70. doi:10.4161/nucl.1.1.10515.

Percipalle, P. 2013. Co-transcriptional nuclear actin dynamics. *Nucleus*. 4:43–52. doi:10.4161/nucl.22798.

Plessner, M., M. Melak, P. Chinchilla, C. Baarlink, and R. Grosse. 2015. Nuclear F-actin formation and reorganization upon cell spreading. *J. Biol. Chem.* jbc.M114.627166. doi:10.1074/jbc.M114.627166.

del Rio, A., R. Perez-Jimenez, R. Liu, P. Roca-Cusachs, J.M. Fernandez, and M.P. Sheetz. 2009. Stretching single talin rod molecules activates vinculin binding. *Science*. 323:638–641. doi:10.1126/science.1162912.

Roux, K.J., D.I. Kim, M. Raida, and B. Burke. 2012. A promiscuous biotin ligase fusion protein identifies proximal and interacting proteins in mammalian cells. *J. Cell Biol.* 196:801–810. doi:10.1083/jcb.201112098.

Seifert, C., and F. Gräter. 2013. Protein mechanics: How force regulates molecular function. *Biochim. Biophys. Acta - Gen. Subj.* 1830:4762–4768. doi:10.1016/j.bbagen.2013.06.005.

Shimi, T., M. Kittisopikul, J. Tran, A.E. Goldman, S.A. Adam, Y. Zheng, K. Jaqaman, and R.D. Goldman. 2015. Structural organization of nuclear lamins A, C, B1, and B2 revealed by superresolution microscopy. *Mol. Biol. Cell*. 26:4075–4086. doi:10.1091/mbc.E15-07-0461.

Shumaker, D.K., K.K. Lee, Y.C. Tanhehco, R. Craigie, and K.L. Wilson. 2001. LAP2 binds to BAF·DNA complexes: Requirement for the LEM domain and modulation by variable regions. *EMBO J.* 20:1754–1764. doi:10.1093/emboj/20.7.1754.

Solovei, I., A.S. Wang, K. Thanisch, C.S. Schmidt, S. Krebs, M. Zwerger, T. V. Cohen, D. Devys, R. Foisner, L. Peichl, H. Herrmann, H. Blum, D. Engelkamp, C.L. Stewart, H. Leonhardt, and B. Joffe. 2013. LBR and lamin A/C sequentially tether peripheral heterochromatin and inversely regulate differentiation. *Cell*. 152:584–598. doi:10.1016/j.cell.2013.01.009.

Stuurman, N., S. Heins, and U. Aebi. 1998. Nuclear lamins: their structure, assembly, and interactions. *J. Struct. Biol.* 122:42–66. doi:10.1006/jsbi.1998.3987.

Stüven, T., E. Hartmann, and D. Görlich. 2003. Exportin 6: a novel nuclear export receptor that is specific for profilin.actin complexes. *EMBO J.* 22:5928–5940. doi:10.1093/emboj/cdg565.

Swift, J., I.L. Ivanovska, a. Buxboim, T. Harada, P.C.D.P. Dingal, J. Pinter, J.D. Pajerowski, K.R. Spinler, J.-W. Shin, M. Tewari, F. Rehfeldt, D.W. Speicher, and D.E. Discher. 2013. Nuclear Lamin-A Scales with Tissue Stiffness and Enhances Matrix-Directed Differentiation. *Science (80-.).* 341:1240104–1240104. doi:10.1126/science.1240104.

Tang, C.W., A. Maya-Mendoza, C. Martin, K. Zeng, S. Chen, D. Feret, S. a Wilson, and D. a Jackson. 2008. The integrity of a lamin-B1-dependent nucleoskeleton is a fundamental determinant of RNA synthesis in human cells. *J. Cell Sci.* 121:1014–1024. doi:10.1242/jcs.020982.

Tapley, E.C., and D. a. Starr. 2013. Connecting the nucleus to the cytoskeleton by SUN-KASH bridges across the nuclear envelope. *Curr. Opin. Cell Biol.* 25:1–6. doi:10.1016/j.ceb.2012.10.014.

Tse, J.R., and A.J. Engler. 2010. Preparation of hydrogel substrates with tunable mechanical properties. *Curr. Protoc. Cell Biol.* 1–16. doi:10.1002/0471143030.cb1016s47.

Wakatsuki, T., M.S. Kolodney, G.I. Zahalak, and E.L. Elson. 2000. Cell mechanics studied by a reconstituted model tissue. *Biophys. J.* 79:2353–2368. doi:10.1016/S0006-3495(00)76481-2.

Wells, R.G. 2013. Tissue mechanics and fibrosis. *Biochim. Biophys. Acta*. 1832:884–90. doi:10.1016/j.bbadis.2013.02.007.

Worman, H.J., J. Yuan, G. Blobel, and S.D. Georgatos. 1988. A lamin B receptor in the nuclear envelope. *Proc. Natl. Acad. Sci. U. S. A.* 85:8531–4.

Yeung, T., P.C. Georges, L. a. Flanagan, B. Marg, M. Ortiz, M. Funaki, N. Zahir, W. Ming, V. Weaver, and P. a. Janmey. 2005. Effects of substrate stiffness on cell morphology, cytoskeletal structure, and adhesion. *Cell Motil. Cytoskeleton*. 60:24–34. doi:10.1002/cm.20041.

Yip, A.K., K. Iwasaki, C. Ursekar, H. MacHiyama, M. Saxena, H. Chen, I. Harada, K.H. Chiam, and Y. Sawada. 2013. Cellular response to substrate rigidity is governed by either stress or strain. *Biophys. J.* 104:19–29. doi:10.1016/j.bpj.2012.11.3805.